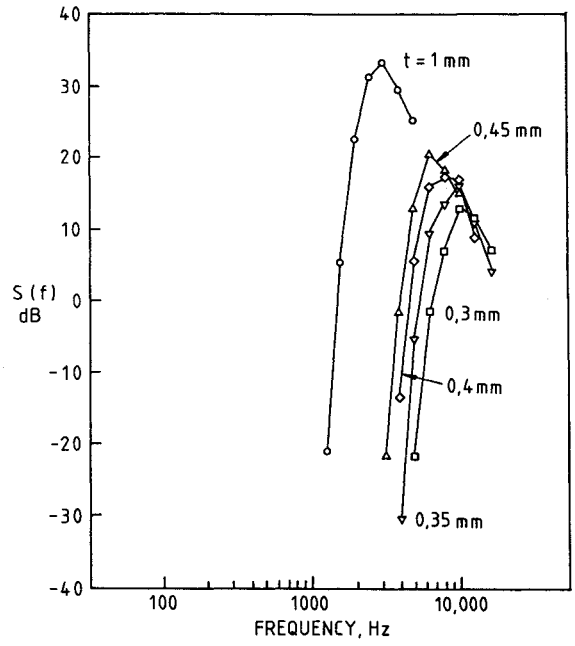

Fig. 4 Effect of trailing-edge thickness on rotor broadband noise.

other sources like in-flow turbulence noise, trailing edge noise, and tip vortex formation noise.

Figure 3 shows the comparison of the analysis to the low-speed fan noise experiment of Lowson et al.[6] Again, all possible broadband noise sources are included. The results show excellent agreement with the experiment.

Figure 4 shows the effect of trailing-edge thickness on rotor broadband noise. Calculations were made based on the low-speed fan as used in Lowson's experiments. It is clear that trailing-edge thickness is a very important parameter for the rotor noise problem. Generally speaking, the noise spectra due to turbulent vortex shedding from blunt trailing edges are peaks occurring at various frequency ranges. The peak frequency depends on the trailing-edge thickness; a small trailing-edge thickness will generate a high-frequency peak, and a thick trailing edge will result in a peak of lower frequencies. The level of the spectrum peak also depends on the thickness of the trailing edge; the peak level increases roughly according to the third power of trailing-edge thickness.

In conclusion, turbulent vortex shedding noise from blunt trailing edges is a very important broadband noise source for rotors. A slightly blunted rotor trailing edge can contribute significantly to the overall noise spectrum. Present analysis provides reasonable predictions for such mechanisms. More accurate prediction could be achieved with better empirical expression for $S_0(\tilde{\omega})$, the normalized spectrum. Clearly, more measurements of surface pressure fluctuations near blunt trailing edges are needed.

Acknowledgment

This work was supported by NASA Langley Research Center, Dr. F. Farassat, Technical Monitor.

References

[1]Schlinker, R. H. and Brooks, T. F., "Progress in Rotor Broadband Noise Research," Paper A-82-38-51D, presented at the 38th Annual Forum of the American Helicopter Society, May 1982.

[2]Brooks, T. F. and Hodgson, T. H., "Prediction and Comparison of Trailing Edge Noise Using Measured Surface Pressures," AIAA Paper 80-0977, June 1980.

[3]Kim, Y. N. and George, A. R., "Trailing-Edge Noise from Hovering Rotors," *AIAA Journal*, Vol. 20, Sept. 1982, pp. 1167-1174.

[4]George, A. R. and Chou, S.-T., "Broadband Rotor Noise Analyses," NASA CR-3797, April 1984.

[5]Hubbard, H. H., Shepherd, K. P., and Grosveld, F. W., "Sound Measurements of the MOD-2 Wind Turbine Generator," NASA CR-165752, July 1981.

[6]Lowson, M. V., Whatmore, A., and Whitfield, C. E., "Source Mechanisms for Rotor Noise Radiation," Department of Transport Technology, Loughborough University of Technology, Loughborough, England, Rept. TT-7202, Feb. 1972.

Turbulent Boundary-Layer Modification by Surface Riblets

E. V. Bacher*
AT&T Bell Laboratories, Whippany, New Jersey
and
C. R. Smith†
Lehigh University, Bethlehem, Pennsylvania

Introduction

In the past several years, significant efforts have been made to develop passive techniques that result in a net reduction in surface shear stress due to boundary-layer turbulence. One technique that demonstrated net surface drag reduction and has the potential for practical aerodynamic and hydrodynamic applications is the use of streamwise triangular V-grooves or riblet surface modifications. Extensive wind tunnel investigations at NASA Langley[1-3] have shown that when these riblets are reduced in size to less than 30 viscous lengths in height and span, surface drag reductions of up to 8% can be achieved.[2] However, despite this apparent success of the riblets in reducing surface drag, it is still unclear how this type of surface affects the fluid interaction with the surface.

The present Note reports on the results of a flow visualization study that examined the most promising drag-reducing riblet surface configuration and attempts to determine changes in the turbulent flow structure precipitated by the riblet surface relative to a conventional flat-plate flow.

Experimental Facility

The experiments were conducted using the Lehigh University free-surface, visualization water channel and high-speed video viewing system described in Ref. 4. Streamwise, triangular riblets were machined on a removable 0.15×1.21 m Plexiglass insert, which began 0.91 m from the leading edge of the test plate shown in Fig. 1. The riblets were triangular in cross section, 1.6 mm deep by 1.6 mm wide, providing optimal nondimensional riblet height and spacing of $h^+ = s^+ = 15$ for 0.21 m/s freestream velocity (see Refs. 5 and 6 for further construction details). The insert was inset such that the peaks of the riblets are flush with the test plate. The side-by-side arrangement of the unmodified and riblet surfaces allowed comparative studies to be performed without realignment of the test plate or readjustment of the channel velocity. A three-dimensional flow trip, designed

Received Feb. 12, 1985; presented as Paper 85-0548 at the AIAA Shear Flow Control Conference, Boulder, CO, March 12-14, 1985; revision submitted Nov. 18, 1985.

*Research Engineer.
†Professor, Department of Mechanical Engineering and Mechanics.

and verified in Ref. 5, was used to initiate the turbulent boundary layer.

Experimental Results

The thrust of the present study was to employ detailed flow visualization to examine the modifications of the turbulent flow structure caused by the riblets; companion hot-film anemometry results are presented elsewhere.[5,6] The nondimensionalized locations and scales cited in this study are based on shear velocities determined from these hot-film data.[5,6] Note that all distances normal to the riblet surface are referenced to the peak of the riblets.

Dye Visualization

At a freestream velocity of 0.21 m/s ($Re_\theta = 900$ at the beginning of the riblet surface), a 1:10 mixture of blue food coloring and channel water was injected simultaneously through transverse surface slots located at the same streamwise location on both the flat and riblet test surfaces (see Fig. 2 for examples). Several differences in the comparative behavior were noted: 1) low-speed streak structures were observed to undulate less freely in the spanwise direction above the riblet surface; 2) very little lateral spreading of the dye was observed near the surface; 3) spanwise streak spacing appeared to be larger above the riblet surface than above the flat surface; 4) concentrations of the dye appeared much darker above the flat plate than above the riblets; and 5) when injection was stopped simultaneously from both slots, the dye persisted in the riblet grooves for a significantly longer time than that on the flat surface. Upon the termination of dye injection, the flat plate appeared to clear of dye within 20 s ($\Delta t^+ = 2000$), while some dye was visible in the grooves up to 2 to 3 min ($\Delta t^+ = 12{,}000$-$18{,}000$) later. The long residence time for the dye within the grooves agrees with the dye visualization studies reported in Refs. 6 and 7, where the dye injected into a single riblet groove tended to remain within that groove.

Hydrogen Bubble Visualization

Both plan- and side-view hydrogen bubble studies were done. Appreciable differences in the side-view studies were not clearly apparent,[5] with the flow behavior above the riblet and corresponding flat plate appearing quite similar, reflecting the characteristic bursting behavior observed previously with hydrogen bubble wires.

The plan-view visualizations were performed at two streamwise locations: 1) $Xp = 60$ cm, the midpoint of the riblet surface; and 2) $Xp = 125$ cm, 5 cm downstream from the termination of the riblet surface. Note that Xp refers to streamwise distances from the beginning of the riblet insert. At each streamwise location, scenes were recorded above both the flat and riblet surface using a high-speed video system.[4,8] Careful slow-motion replay of the recorded scenes allowed detailed evaluation of the flow behavior.

General Observations

At $Xp = 60$ cm, the bubble-wire height was varied systematically from a nondimensional viscous height of $y^+ = 50$ to 0. Above $y^+ = 15$, there was little apparent difference between the streaky structure developing above the flat and riblet surfaces. Below $y^+ = 15$, the lateral movement of the streaks above the riblet surface appeared to decrease markedly compared with the lateral movement observed above the flat surface (where sinuous, lateral motion is a common characteristic); the closer the wire was placed to the riblets, the more the lateral activity level decreased relative to that observed above the flat surface. In addition, it appears that the low-speed regions are less concentrated above the riblet surface (implied by a reduced brightness due to a weaker concentration of bubbles—see Fig. 3), indicating that

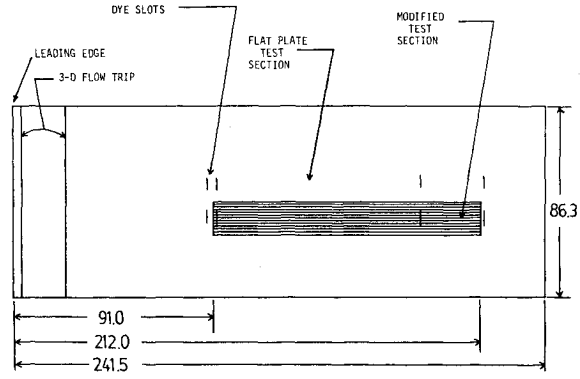

Fig. 1 Test plate used in present study (dimensions in centimeters).

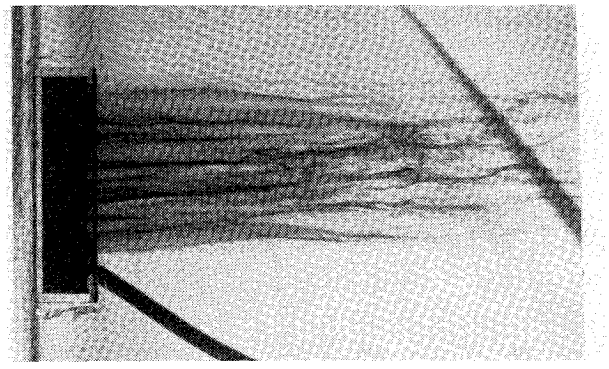

a) Flat plate.

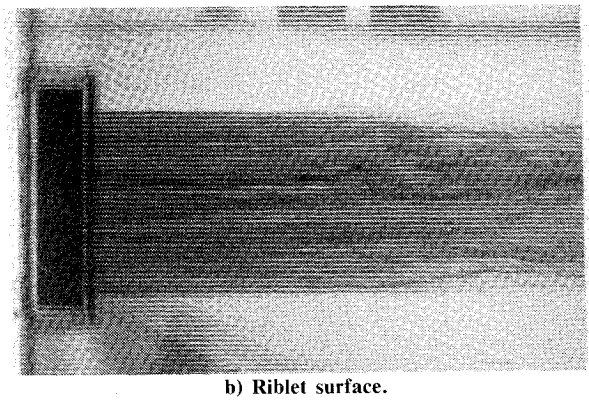

b) Riblet surface.

Fig. 2 Plan-view photographs showing comparative dye-slot visualization. $Re_\theta = 1200$, slots at $Xp = 94$ cm.

spanwise velocity effects due to low-speed streak formation are less severe above the riblets; this was confirmed using single bubble time lines, which demonstrated a much gentler spanwise kinking as compared to time lines at comparable heights above the flat surface. At the closest wire position to the riblets, the wire actually touched the riblet peaks, with the bubbles above the riblet valleys markedly decelerating, such that the bubble lines appear to conform to the riblet shape.

At $Xp = 125$ cm, the bubble-wire height was varied from $y^+ = 20$ to 0 in order to determine if the effect of the riblet surface persisted beyond the streamwise extent of the grooves. It was observed[5] that the lateral movement of the streaky structure quickly returns as the boundary layer leaves the riblet surface.

Streak Spacing

Streak counts were made at streamwise locations of $Xp = 60$ and 125 cm for a nondimensional wire height of

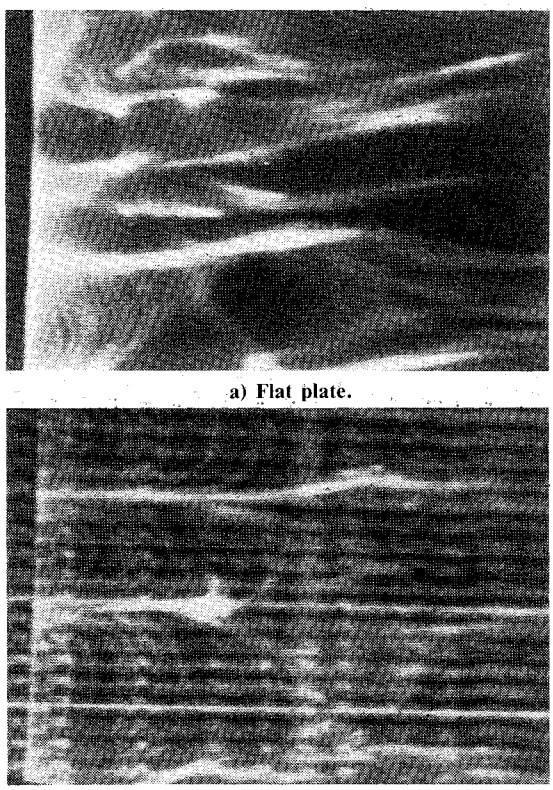

a) Flat plate.

b) Riblet surface.

Fig. 3 Planviews of low-speed streaks, hydrogen bubble visualization ($Xp = 60$ cm, $Re_\theta = 1200$).

$y^+ = 5$. The momentum thickness Reynolds numbers at these locations (for the flat-plate section) were: $Re_\theta = 1200$ for $Xp = 60$ cm and $Re_\theta = 1350$ for $Xp = 125$ cm. The criterion for streak identification was that employed in Ref. 8.

For the flat plate at $Xp = 60$ cm, a nondimensional streak spacing of $\bar{\lambda}^+ = \bar{\lambda} u_\tau / \nu = 93$ was determined. This is in good agreement with the results of Refs. 4 and 8 for flat-plate flows. The mean nondimensional streak spacing above the riblet surface at the same streamwise location and flow condition was 135, representing an increase of 45% relative to the flat-plate spacing. Reference 7, using spatial correlations from two hot-film probes, also reported an increase in the streak spacing above a riblet surface of 15-30% over the flat-plate value.

Streak counts taken at $Xp = 125$ cm indicate a mean nondimensional streak spacing $\bar{\lambda}^+ = 98$ for the flat plate and $\bar{\lambda}^+ = 140$ for the riblet surface. Since this count took place 5 cm downstream of the termination of the riblet insert, it is apparent that there is a persistence of the modifying effects of the riblets. It should be recalled that the video scenes indicate that lateral activity increases markedly once the flow leaves the riblet surface. This suggests that, although the larger streak spacing persists for some distance after the end of the riblets, the return of elevated lateral communcication may cause the boundary layer to relax back toward the flat-plate characteristics.

The present visualization studies confirm that the flow within the riblets is slow and quiescent; in addition, they show that the low-speed streak structure exists and does draw fluid from the grooves. The increased streak spacing and apparent increase in flow uniformity above the riblet surface in comparison to the flat plate implied that there are fewer regions of instability and that those regions may behave more weakly in implementing exchange of momentum between the near-wall and the outer region of turbulent boundary layers. This suggestion appears to be borne out by the companion anemometry results presented in Refs. 5 and 6.

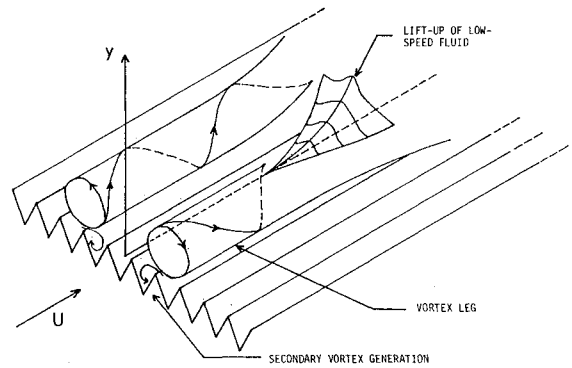

Fig. 4 Perspective schematic showing the hypothesized interaction of counterrotating streamwise vortices in the wall region of a turbulent boundary layer with a riblet surface.

Discussion

As discussed in detail in Refs. 5 and 6, it is suggested that the effect of the riblets is to modify and effectively reduce the momentum exchange properties caused by the streamwise vortices developing near the surface beneath a turbulent layer, with a consequent reduction in the surface shear stress. It is thought that an important action of the sharp-peaked riblets is to limit spanwise concentration of low-speed fluid. It is suggested that this is accomplished by a mechanism which relys on secondary vortex generation.[9]

A schematic drawing in Fig. 4 illustrates the hypothesized interaction of the riblets with a pair of counterrotating streamwise vortices. Note that the generation of secondary vortices at the riblet peaks serves two functions: weakening of the streamwise vortices, and inhibiting the spanwise concentration of low-speed fluid into streak formations. Inhibiting streak formation (i.e., increasing streak spacing) should decrease the number of "burst" sites, which will inhibit turbulent momentum exchange in the boundary layer. This process enables the riblet surface to retard the development of the turbulent boundary layer and thus to reduce the surface drag. For a more detailed development of this model and discussion of the implications with regard to riblet drag reduction, the reader is referred to Refs. 5 and 6.

Acknowledgments

The authors would like to thank the U.S. Air Force Office of Scientific Research and Dr. Michael Francis, contract monitor, for support of this research.

References

[1]Walsh, M. J., "Drag Characteristics of V-Groove and Transverse Curvature Riblets," *AIAA Progress in Astronautics and Aeronautics: Viscous Drag Reduction*, Vol. 72, edited by G. R. Hough, AIAA, New York, 1980, p. 168.

[2]Walsh, M. J., "Riblets as a Viscous Drag Reduction Technique," *AIAA Journal*, Vol. 21, April 1983, pp. 485-486.

[3]Walsh, M. J. and Lindemann, A. M., "Optimization and Application of Riblet for Turbulent Drag Reduction," AIAA Paper 84-0347, 1984.

[4]Johansen, J. B. and Smith, C. R., "The Effects of Cylindrical Surface Modifications on Turbulent Boundary Layers," *AIAA Journal*, Vol. 24, July 1986, pp. 1081-1087.

[5]Bacher, E. V. and Smith, C. R., "An Experimental Study of the Modifying Effects of Streamwise Grooved Surface of Triangular Cross-Section on the Flow Structure and Statistical Characteristics of Turbulent Boundary Layers," Dept. of Mechanical Engineering, Lehigh Univesity, Bethleham, PA, Rept. FM-7, 1985.

[6]Bacher, E. V. and Smith, C. R., "A Combined Visualization-Anemometry Study of the Turbulent Drag Reducing Mechanisms of Triangular Micro-Groove Surface Modifications," AIAA Paper 85-0548, 1985.

[7]Gallagher, J. A. and Thomas, A.S.W., "Turbulent Boundary Layer Characteristics over Streamwise Grooves," AIAA Paper 84-2185, 1985.
[8]Smith, C. R. and Metzler, S. P., "The Characteristics of Low-Speed Streaks in the Near-Wall Region of a Turbulent Boundary Layer," *Journal of Fluid Mechanics*, Vol. 129, 1983, p. 27.
[9]Doligalski, T. L. and Walker, J.D.A., "The Boundary Layer Induced by a Convected Two-Dimensional Vortex," *Journal of Fluid Mechanics*, Vol. 139, 1984, p. 1.

Observations on the Structure of an Edge-Tone Flowfield

A. Krothapalli*
The Florida State University, Tallahassee, Florida
and
W. C. Horne†
NASA Ames Research Center
Moffett Field, California

Introduction

An edge tone is the sound of a discrete frequency produced by a thin rectangular jet of fluid impinging on a wedge. Edge tones were discovered in 1854 by Sondhaus and have been the subject of a large number of experimental and theoretical investigations. An admirable review of these is given by Karamcheti et al.[1] The wedge is essential to edge-tone generation because the tone does not appear when the wedge is removed from the jet. The nature of the flow processes occurring at the wedge is therefore an important factor in edge-tone production. The interaction region of the flow at the edge has also been used to illustrate the leading-edge "Kutta condition." The detailed features of the unsteady flow at the edge, however, are still to be understood. A discussion of the Kutta condition in unsteady leading-edge flows is given by Crighton,[2] who suggested that the best illustration of such flow is afforded by the edge-tone configuration. With this in mind, an experiment was conducted to examine the unsteady flowfield in the interaction region of the jet with the leading edge of the wedge.

The main parameters or variables governing the problem are the Mach number and Reynolds number of the jet near the exit, the state of the flow at the exit of the nozzle, the geometry and disposition of the wedge with respect to the nozzle exit, and the condition of the ambient medium into which the jet is issuing. The present experiment was conducted in two parts. The first part of the investigation deals with a high-speed subsonic jet ($M=0.8$) impinging on a 20-deg wedge. The second part of the investigation deals with more detailed measurements of the flowfield, using a low-speed subsonic jet ($M=0.23$) impinging again on a 20-deg wedge. The Reynolds number employed was based on the width of the nozzle and was about 5×10^4 for the high-speed case; for the low-speed jet case, it was about 3×10^4. From the measurements of the mean velocity at the nozzle exit, top-hat mean velocity profiles are observed for the two cases tested.

Received Oct. 15, 1985; revision received Dec. 9, 1985.

*Associate Professor, Department of Mechanical Engineering, Florida A&M University/FSU College of Engineering. Member AIAA.
†Aerospace Engineer, Lowspeed Aircraft Research Branch. Member AIAA.

Apparatus, Instrumentation, and Procedure

Experiments described here were conducted at two different times and in two different laboratories. However, when similar parameters were used, both experiments gave similar results. The detailed flow measurements were made using a low-speed jet ($M=0.23$) facility at NASA Ames Research Center. For other measurements, the blowdown facility at Stanford University was used. In the first case, the dimensions of the rectangular exit of the nozzle used were 50 mm long (L) and 3 mm wide (D), and were preceded by a 40-mm-long, smooth, rectangular channel (50 mm × 3 mm). The experimental facility and model are described in detail by Krothapalli and Horne.[3] A 20-deg wedge was selected here because of its use in early Stanford investigations.

A B&K type 4138 microphone (3 mm diam), which has a flat response to about 100 kHz, was used o make the acoustic measurements. The microphone was calibrated using a B&K type 4220 Pistonphone. The location of the microphone was held fixed with respect to the leading edge of the wedge throughout the experiment.

A self-synchronizing schlieren system employing a phase-locked technique was used for flow visualization. The schlieren image of the flowfield was displayed on a ground-glass screen for visual observation or on a film to obtain a photographic record. Schlieren photographs were taken using Polaroid-type 57 instant film (ASA 3000).

The velocity field and surface pressure distribution of a low-speed edge tone were measured at the anechoic chamber facility at Ames Research Center. A rectangular nozzle having dimensions of 0.508 cm × 10.16 cm was used. A 20-deg aluminum wedge was provided with 10 pressure transducer ports and could be positioned at arbitrary distances from the nozzle exit with a lead screw. It was found that multiple nonharmonic tones were generated over most of the operating range of this apparatus. In order to simplify the data sampling procedure, the conditions $M=0.23$ and $h/d=6.25$ were selected for study since only harmonically related tones were observed.

The velocity field was surveyed with a miniature X-wire probe equipped with platinum-coated tungsten sensors 5 μm in diameter and 1 mm long. The probe was operated in the constant temperature mode, which ensured accurate phase response to 3 kHz. Fluctuating surface pressures were measured with 0.48-cm-diam transducers embedded in the wedge and connected to the pressure ports via 0.128-cm-diam passages. The diameter of the pressure port at the surface was 0.064 cm. The intersection of the tip port with the edge produced a 0.064-cm width by 0.02-cm-long notch at the central region of the wedge. All measurements were conditionally sampled on the basis of the phase of one of the surface pressure transducers. A detailed description of the apparatus and procedure is given in Refs. 3 and 4.

Results and Discussion

Flow Visualization

Typical sequences of phase-locked schlieren pictures of the edge-tone flowfield for two different edge heights at an exit Mach number of 0.8 are shown in Fig. 1. The knife edge of the schlieren system is oriented parallel to the jet axis. The signal form the near-field microphone was used to trigger the light source. The wedge in Figs. 1a and 1b is positioned such that the edge tone operates in stage 1 and stage 2 modes, respectively. The time interval between two successive pictures during stage 1 operation is 25 μs, while during stage 2 operation, it is 20 μs. The figure shows the similarity of the overall flowfield for the two cases.

From the sequence of pictures, the following observations are made. Large-scale vortical structures, referred to here as primary vortices, can be identified in the shear layers on either side of the jet, and these grow in intensity as the jet approaches the wedge. At the leading edge, a secondary